IEEE/CSC & ESAS EUROPEAN SUPERCONDUCTIVITY NEWS FORUM, No. 19, January 2012
Submitted to ESNF Nov. 16, 2011; accepted Nov. 30, 2012. Reference No. ST286, Category 6
The published version of this manuscript appeared in *IEEE Trans. Appl. Supercond.* **22**, (4003106) (2012)

Limits to high field magnets for particle accelerators

E. Todesco, P. Ferracin

***Abstract* — What is the ultimate limit to high fields in superconducting magnets for particle accelerators? In this paper we review the present status of the technology, outlining the main limitations. We first analyse the needed margin for operating a magnet in an accelerator. We then review the relation between current densities, coil widths, and fields in the magnets build so far. The issue of stress and the dependence on the coil lay-out is then discussed: a careful optimization between current density and coil width can be needed to keep the forces and associated strain within acceptable limits. The main issues related to cable lay-out (strand diameter, filament size) are then discussed. We conclude by giving a hint on the requirements on a HTS conductor, and a summary of Nb-Ti and Nb_3Sn.**

***Index Terms*—superconducting accelerator magnets, dipoles, quadrupoles, low-temperature superconductors**

I. Introduction

The quest for higher and higher fields in accelerator magnets is a good paradigm of advancement in science and technology. On the one hand, superconducting magnets allowed increasing the bore magnetic field of one order of magnitude, from the ~1.5-2 T limit of resistive magnets to the world record of nearly 14 T in a sizeable bore [1]. On the other hand, the progress since the first accelerator magnets in the 70's [2], [3] may look slow: 4 T in Tevatron at the beginning of the 80's, 5 T in Hera in the 90's, and 8 T still to reach for the Large Hadron Collider operation.

Nb_3Sn has the potential to be the workhorse of the 21st century accelerators, but a magnet made with this technology with all the features necessary for reliable operation is still to come. What is clear is that a considerable work is needed to achieve results: every additional tesla is gained with considerable efforts, trials and errors, and without massive research programs nothing happens. Nature does not make presents in this field. Nevertheless, the experience from solenoids [4] shows that the potential is there, and a considerable performance is at hand. In these pages we will summarize the present status of high field magnets for accelerators, pointing out the main open issues.

II. Margin

The maximum performance reachable by a superconducting magnet is estimated through (i) an electromagnetic (e.m.) model of the conductor lay-out and (ii) critical current measurements of the superconducting strand and/or cable. The e.m. model provides the so-called *loadline*, i.e. the relation current density versus bore/peak field in the coil – this is a straightforward estimate based on Biot-Savart law and on a finite element model for the iron saturation if this is relevant. On the other hand, the cable performances in terms of critical current are much more difficult to estimate, and are affected by an error which can easily reach 5% for Nb-Ti, and even more for Nb_3Sn and HTS due to strain sensitivity.

The intersection of the loadline with the critical surface provides the maximum performance of the magnet (see Fig. 1), usually called *short sample* limit. Never forget that due to the limited knowledge of the critical surface of the superconductor within the magnet, this quantity is known at most within 5%.

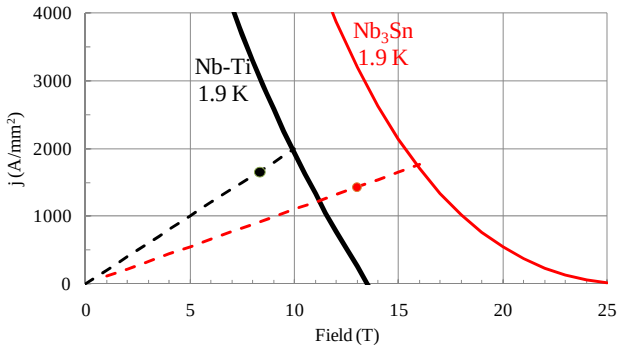

Fig. 1: j_{sc} versus B for Nb-Ti and Nb_3Sn at 1.9 K, loadlines for 8.3 T (LHC dipole) and a possible 13 T dipole, and operational points (dots).

The magnet is not operated at the short sample limit: a margin is needed. For the LHC case, short sample is 9.7 T and operational field is 8.3 T so the *loadline margin* is (9.7-8.3)/9.7=14%. How much margin is really needed is a relevant question: for magnets in the range of 20 T short sample, a 20% margin means 4 T, i.e. the field of the Tevatron dipoles!

In Table I we list the loadline margin for the main magnets used in particle accelerators: values range from 20 to 30%. Tevatron had routine operation at 980 GeV, i.e. 2% lower than nominal, with a 24% margin. HERA energy was increased from 820 to 920 GeV lowering the operational temperature from 4.6 to 3.9 K, and keeping the same 23% margin. RHIC has been built with a comfortable 30% margin. The LHC dipoles were designed with a lower margin – the machine is running today at half of the energy for doubts on the interconnections, but one sector (154 dipoles) has been re-trained up to 6.6 TeV, i.e. 7.8 T field, corresponding to 19% margin, with about 25 quenches. From these data, one can

Manuscript received 12 September 2011.

P.Ferracin is with Lawrence Berkeley Laboratory, E. Todesco is with the CERN Technology Department, 1211 Geneva 23, Switzerland. (e-mail: Ezio.Todesco@cern.ch)

argue that a 20% loadline margin is needed. In reality, what counts for the magnet stability is the temperature and/or the energy margin, depending on the operational conditions: nevertheless, the loadline margin is widely used – and rarely discussed on paper. Here, we will try to address this issue.

TABLE I. MARGIN FOR DIFFERENT ACCELERATORS

	Nominal			Actual		
	Temp. (K)	Field (T)	Margin	Temp. (K)	Field (T)	Margin
Tevatron	4.2	4.3	22%	4.2	4.2	24%
Hera	4.6	4.7	23%	3.9	5.3	23%
RHIC	4.5	3.5	30%	4.5	3.5	30%
LHC	1.9	8.3	14%	1.9	*7.8**	*19%*

* reached in one eight of the LHC during hardware commissioning (no beam)

In the case of continuous losses, one has to ensure that coil does not reach a temperature that puts the operational values of current and field on the critical surface. This is the case of a magnet under the shower of debris coming from the interaction point. Here, the relevant parameter is the *temperature margin*, and the efficiency of the mechanism of heat extraction.

We first consider a family of magnets with different loadlines and 20% margin. We compute for each case the temperature margin using the known parameterizations [5] – [7] for the critical surfaces. Results are shown in Fig. 2: a 20% margin on the loadline corresponds to a temperature margin which weakly depends of the field: for Nb-Ti there is a temperature margin of about 2 K at 1.9 K and 1 K at 4.2 K. For Nb_3Sn, due to the different shape of the critical surface, the margin is larger by a factor ~2.5, giving 4.5 K to 5.5 K at T_{op}=1.9 K and 3.5 K to 4 K at T_{op}=4.2 K.

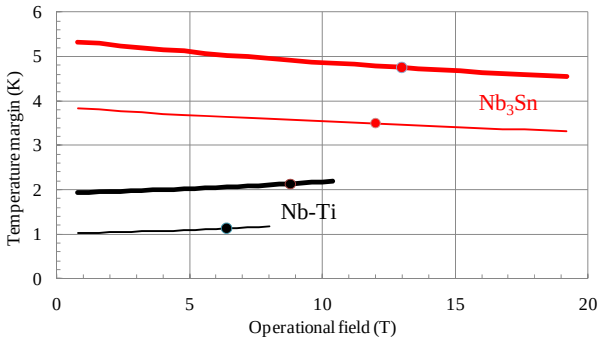

Fig. 2: Temperature margin versus operational field for Nb-Ti and Nb_3Sn at 1.9 K (thick lines) and 4.5 K (thin lines) – case of 20% loadline margin.

For instantaneous losses, all the heat remains in the coil, and one has to ensure that the energy deposited does not increase the temperature of the conductor beyond the critical surface. Therefore, what counts is the *energy margin*. This is the case of instantaneous beam losses along the ring, or energy deposited by coil movements induced by electromagnetic forces. Using the specific heats of a typical cable, one can translate the above temperature margins in energy margins. Results are shown in Table II, where the helium contribution is excluded. For Nb_3Sn specific heat we use an expression derived in [8]. The estimate depends on the cable, and especially on the copper to non-copper ratio: we considered an LHC cable for Nb-Ti (Cu/Non- Cu=1.65) and the HQ [9] conductor (Cu/Non-Cu=1.17) for Nb_3Sn. For both materials, the 20% loadline margin provides about 1/3 larger energy margin at 4.2 K w. r. t. 1.9 K – therefore this rule makes operation at 1.9 K more challenging than at 4.2 K.

The comparison between Nb-Ti and Nb_3Sn also shows that the latter one has about a factor four more in energy margin. Unfortunately, this does not imply that the 20% loadline margin used in Nb-Ti can become 5% for Nb_3Sn, since other aspects have also to be considered (see next sections).

Helium plays a fundamental role when it permeates the coil, as in Nb-Ti non-impregnated coils. Taking into account of this effect, the energy margin increases by one order of magnitude.

The two extreme cases considered there - continuous losses and instantaneous losses show that in the first case the specific heats of the conductor is not relevant, and what counts is the temperature margin and the mechanism of heat removal. In the second case the specific heats of the coil, including superfluid helium if present, play the key role. In both cases, it is hard to give a quantitative justification of the 20% loadline margin.

TABLE II TEMPERATURE MARGIN AND ENERGY MARGIN FOR NB-TI AND NB_3SN AT 1.9 K AND 4.2 K WITH 20% LOADLINE MARGIN

	Oper. temp.	Short sample field	Oper. field	Loadline margin	Temp. margin	Energy margin
	(K)	(T)	(T)		(K)	(mJ/cm^3)
Nb-Ti	4.2	8.0	6.4	20%	1.13	4.1
Nb-Ti	1.9	10.0	8.0	20%	2.13	3.2
Nb_3Sn	4.2	12.0	9.6	20%	3.50	15.6
Nb_3Sn	1.9	13.0	10.4	20%	4.75	11.4

III. CURRENT DENSITY AND COIL SIZE

In a dipole having a sector coil of width w, without copper wedges, the central field is given by

$$B = \kappa_d \, j_o \, w \qquad (1)$$

where j_o is the *overall current density*, i.e. including the stabilizer in the strand, voids and structural material which are part of the coils. The term engineering current density, widely used, usually does not include insulation. If j_o is given in A/mm^2 and w in mm, for a 60° sector coil one has κ_d=0.69 × 10^{-3} T mm/A [10]. In a quadrupole one has a similar equation for the field gradient

$$G = \kappa_q \, j_o \log\left(1+\frac{w}{r}\right) \qquad (2)$$

where r is the aperture radius and κ_q=0.69 in the horrible but very practical units (T/m)/ (A/mm^2) [11]. These equations can be generalized to include the influence of the iron, but we use ironless approximations to have a first order guess of the main parametric dependence.

The presence of copper wedges in the coil can be taken into account by defining an *equivalent coil width* w_{eq} which is the width of a 60° sector having the same cross section surface A of the coil [10]:

$$w_{eq} \equiv r\left[\sqrt{1+\frac{3A}{2\pi r^2}}-1\right]. \qquad (3)$$

The equivalent coil width is in general around 10-15% smaller than the total width of the coil in a cosθ lay out. For instance in the LHC dipole one has a coil width of 30.8 mm (2 layers of 15.4 mm width insulated cable) and the w_{eq}=26.9 mm. The same equation holds for a quadrupole, where a 30° sector is considered. The main advantage of this definition is that it allows a direct comparison between cosθ and block lay-outs.

The two obvious paths to high field and high gradients are *larger current densities* and/or *larger coils*. In Fig. 3 we show the relation between bore field and coil width for the main Nb-Ti accelerator magnets (operational field) and for some Nb_3Sn models. To be fair to the glorious Nb-Ti, for Nb_3Sn models 80% of the short sample is taken at 1.9 K. One finds that notwithstanding the different designs and the two superconducting materials, current density is typically around 400 A/mm^2 (see Fig. 4). Please note that for graded magnets one has two values corresponding to the densities in inner and outer layer, the outer being the larger value.

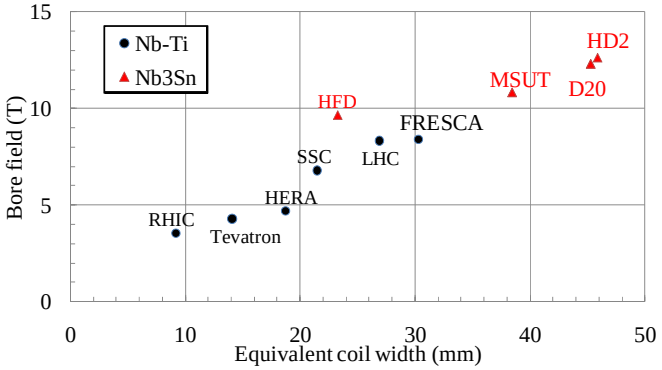

Fig. 3: Operational field versus coil size – dipoles (80% of short sample at 1.9 K for Nb_3Sn models and for Fresca facility).

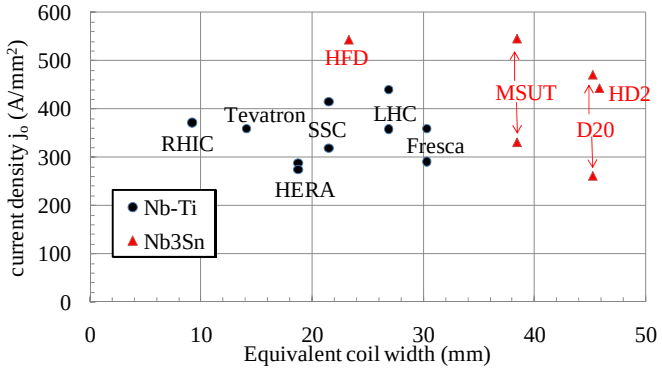

Fig. 4: Operational overall current density versus coil size – dipoles (80% of short sample at 1.9 K for Nb_3Sn models and for Fresca facility).

Considering that the fraction of superconductor in an insulated coil can range from one third to one fourth, this means to have the superconductor operating at 1200 A/mm^2 - 1600 A/mm^2. Given the superconductor critical surfaces, this sets a natural limit of ~8 T for Nb-Ti and ~13 T for Nb_3Sn (see Fig. 1).

Critical current in Nb-Ti has been optimized since a long time and it has already reached the maximum limit. For Nb_3Sn there has been a considerable progress [12,13] in the past 10 years. With the present conductor performance, 13 T operational field is close to the limit. Using grading one could possibly reach 15 T with coil widths that are still within 80 mm.

In order to reach the level of 16 T one should improve the current density in that region (optimization has been focused up to now in the 12-15 T region): a very ambitious target of 1500 A/mm^2 at 20 T would allow to get at 16 T operational field with a reasonable size of the coils.

If larger current densities cannot be obtained above 15 T, the alternative is to use lower current densities and larger coil, i.e., reduce the slope of the loadline of Fig. 1. An estimate of the operational field (with 20% margin) versus the coil size is given in Fig. 5, based on the scaling laws presented in [10]. If 40 mm coil gives 12.5 T operational field, doubling the coil width provides only two additional Tesla: the game becomes pretty expensive – with grading on can save about one third of conductor, but to get to operational fields of 15 T with present conductor performances looks at the limit (or probably slightly beyond the limit) of the Nb_3Sn technology.

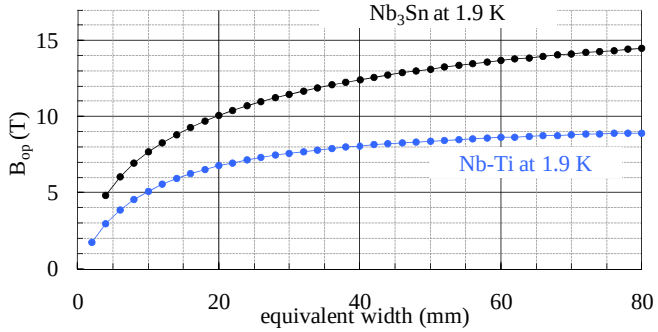

Fig. 5: Operational field versus coil width for a 20% margin from critical surface.

In Fig. 6 and 7 we present the case of the quadrupoles. We plot the gradient versus the factor log(1+*w*/*r*) since this is the term which is proportional to the gradient via the current density (see Eq. 2). The spread in the current density (Nb_3Sn models are again considered with 20% margin on 1.9 K short sample) is more relevant than in dipoles. In particular, the two Nb_3Sn magnets made by the LHC Accelerator Research Program (LARP) are in the range of 600-750 A/mm^2 (see Fig. 7).

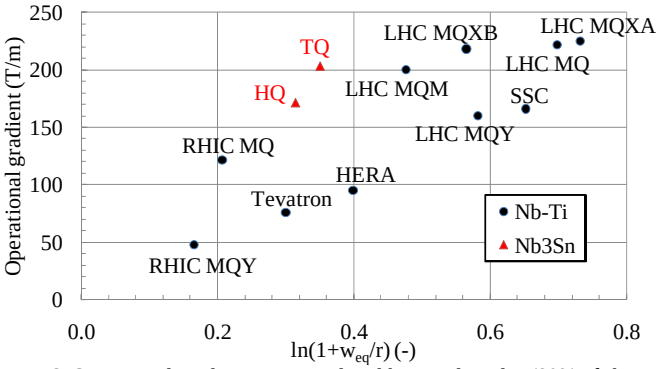

Fig. 6: Operational gradient versus coil width – quadrupoles (80% of short sample at 1.9 K for Nb_3Sn models).

With a few exceptions, Nb-Ti operational current densities are in the range of 300 A/mm^2 to 500 A/mm^2. In general, Nb_3Sn coils provide about 50% larger gradient for the same aperture w. r. t. Nb-Ti [11].

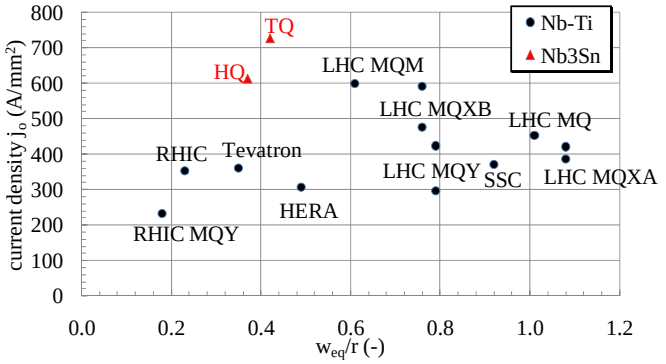

Fig. 7: Overall current density versus coil width – quadrupoles (80% of short sample at 1.9 K for Nb_3Sn models).

IV. FORCES, STRESS, STRAIN

Large current densities provide higher fields or more compact coils. But they induce higher stresses, and stress can be a major issue for two different reasons:

- For the Nb-Ti a soft limit is set by the damage of the insulation of the coil – present types of insulations can withstand up to 200 MPa, and LHC coils during collaring were compressed up to 150 MPa.
- For Nb_3Sn there is a hard limit which is the critical current degradation induced by strain. This limit has a strong dependence on the strand lay-out and fabrication: in some cases measurements have shown significant degradation already at the level of 50-100 MPa. The RRP, which is the workhorse of the LARP, has shown negligible degradation up to more than 150 MPa [14,15]. These measurements are particularly tricky since the real condition of stress of the cable in the magnet is hard to achieve in a sample. A few experiments on magnets, loaded with increasing stress, have shown negligible performance degradation up to 200 MPa [16]. Indeed, the larger stress is on the lower field regions and one should always be extremely careful in generalizing these results.

One can estimate the maximal stress in the midplane for a dipole sector coil according to the following equation [17]

$$\sigma \approx j^2 \frac{\mu_0 \sqrt{3}}{6\pi} \mathrm{Max}_{\rho\in[r,r+w]}\left[2\rho^2 + \frac{r^3}{\rho} - 3\rho(r+w)\right] \quad (4)$$

The stress obviously scales with the square of the current, plus a geometric factor which is a function of the magnet aperture and of the coil width. If we compensate a lower current density with a larger coil width, it turns out that the geometric factor grows slower than j^2: the same field obtained with a lower current density has a significantly lower stress. This is shown in Fig. 8, where the following estimate is carried out: for a given current density and operational field we compute the coil width to reach that field with Eq. (1) and we estimate the stress with Eq. (4).

The LHC main dipole, having 70 MPa stress with 380-420 A/mm^2 current density, fits rather well with the estimate. The 400 A/mm^2 used in many magnets provides a field of 13 T with about 110 MPa, and 150 MPa at 16 T, which is still in the tolerable range. Increasing the current density one can reduce the coil size, but stress becomes larger. For instance, if 200 MPa is considered as the ultimate limit, 400 A/mm^2 give a maximum field of ~20 T whereas with 700 A/mm^2 one stops at ~15 T. The dependence on the aperture is steep but not dramatic: doubling the aperture from 40 to 80 mm at 15 T induces an increase in the stress of about 50% from 120 to 180 MPa (see Fig. 9). Please note that these estimates should be used with a pinch of salt since they neglect the detail of the structure, local stresses, and the need of prestressing the coil: they give an educated guess of midplane stress with a ~20% error, and, what is more precious, the trends for the dependence on the main parameters.

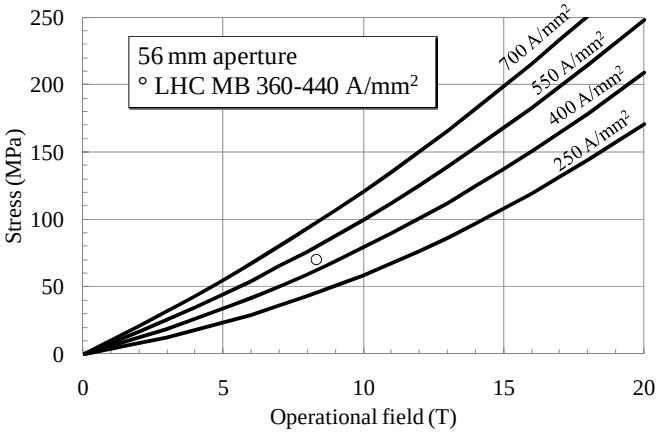

Fig. 8: Midplane stress versus field for different current densities, and 56 mm aperture - dipoles.

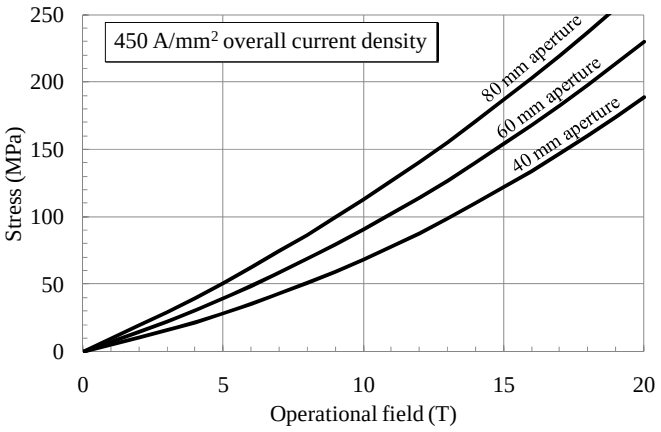

Fig. 9: Midplane stress versus field for different apertures, overall current density 450 A/mm^2 - dipoles.

In quadrupoles one has a similar equation, with a different geometric factor [18]

$$\sigma \approx j^2 \frac{\mu_0 \sqrt{3}}{16\pi} \mathrm{Max}_{\rho\in[r,r+w]}\left[\rho^2 - \frac{r^4}{\rho^2} + 4\rho^2 \ln\left(\frac{r+w}{\rho}\right)\right] \quad (5)$$

but one has different results w.r.t. the dipole case. For a small aperture as the LHC arc quadrupole (56 mm), different current densities give very similar stresses (see Fig. 10). For larger apertures, lower current densities provide lower stresses, but

without the large difference found in the dipole case (see Fig. 11 for the 120 mm case). In both figures we do not show data corresponding to coil widths larger than 100 mm: this is why the curves suddenly stop in some cases. We also added the working point of LHC MQ and LARP HQ, which fit reasonably well in our plot. For quadrupoles, stress is not putting such a tight upper limit to the critical current density as for the dipoles.

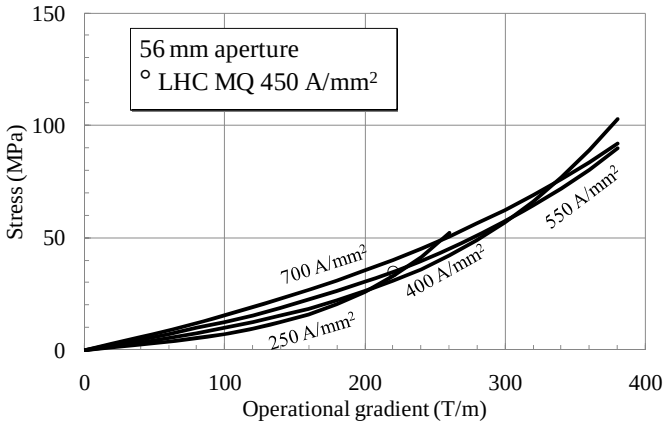

Fig. 10: Stress versus gradient for different current densities, 56 mm aperture.

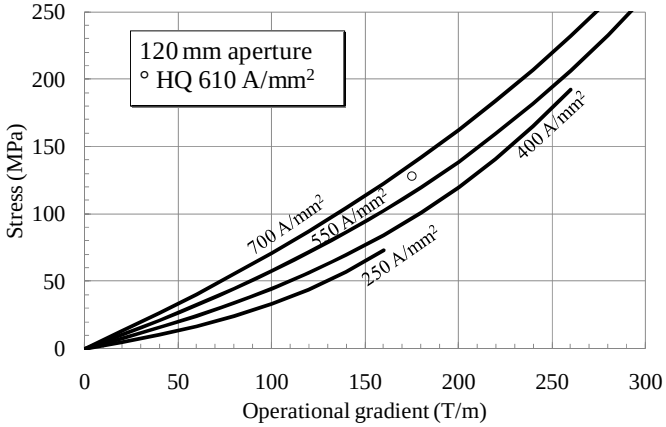

Fig. 11: Stress versus gradient for different current densities, 120 mm aperture – HQ has 600 A/mm2 overall current density (see Fig. 7).

V. Grading and Cost

Grading the current density, i.e. putting a high current density in the outer layer where the field is lower, is a well-known strategy. The main advantage is a considerable decrease of the amount of conductor needed for the outer layer, which brings a reduction in the coil size and in the cost. The drawback is that the stress is increased. Therefore for cases in which the stress is already at the limit, grading is not the right solution: grading looks more appealing for high gradient (or large aperture) quadrupoles than for high field dipoles.

The second possibility is *grading the material*. In this case the current density is kept constant, and the less performing material is placed in the low field region. The coil size is not reduced, but stress does not increase. This grading has a large impact on cost, since there is about a factor five between Nb-Ti and Nb_3Sn, and at least another factor five between Nb_3Sn and a possible HTS conductor for accelerator magnets (which is still under development). Grading the material is a must for a main dipole accelerator magnet above 10 T. This implies hybrid coils, i.e. developing a technology that allows to put together materials with different needs in terms of heat treatments, with different mechanical and thermal properties. Whereas this is done routinely for solenoids, little experience is present in this field: an hybrid Nb-Ti / Nb_3Sn magnet showed that this option is viable but a careful ad hoc design of the structure is needed [19].

VI. The Cable: Protection, Hysteresis, Instabilities and Ramp Rate

Having fixed the material, overall current density, and width of the coil, one has to choose the cable. The copper-non-copper ratio affects the overall current density, and has to be large enough to guarantee protection. Usually it ranges from 1 to 2 in most cases, i.e., 50% to 66% of copper in the strand. A larger quantity of copper also provides a larger energy margin.

The second crucial parameter is the strand diameter. Large strands allow larger cables carrying more current and reducing the inductance. On the other hand, smaller strands can be easier to wind. There is an upper limit to the number of strands and the strand diameter present in a cable – typically 40-50 is already large. Finally, the strand diameter also plays a relevant role for the self-field instabilities, larger diameter strands being less stable [20].

The third relevant parameter is the filament size. If for the strand diameter one has pro and cons for both large and small strands, and the same is for the choice of the copper/non copper ratio, in the case of the filament size the receipt is simple: make it as small as possible. There are a number of different physical effects which scale with the filament size, mainly (i) magnetization, giving a relevant change of transfer function and multipoles difference between injection and high field currents, and (ii) instabilities, limiting quench performance. The first aspect can be less critical for magnets which are dominant only at high field, as the final focus quadrupoles, but the second one is a severe showstopper that blocked a research program for a few years (see HFD01-3 in Fig. 12, [21]): when a new strand with smaller diameter and filament has been adopted the instabilities were cured (see HFD05-7 in Fig. 12).

For the Nb-Ti magnets a size of 5-7 μm can be routinely achieved. On the other hand, Nb_3Sn is still one order of magnitude away from this ambitious target.

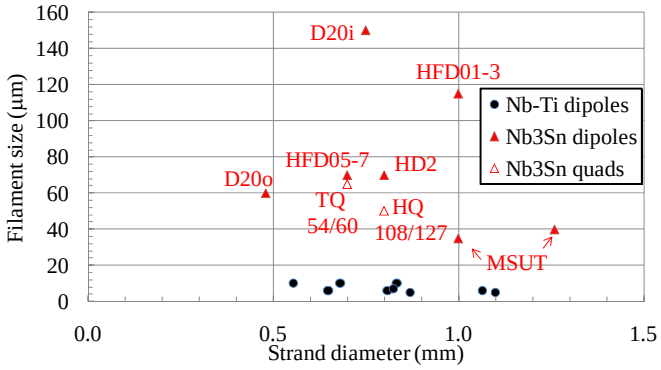

Fig. 12: Filament size versus filament diameter.

The last issue we want to briefly outline is the interstrand resistance. This parameter is related to ramp rate effects induced by current loops in the cable, and in Nb-Ti magnets this can be kept high through oxidizing the strand. This procedure cannot be used for Nb_3Sn: a possible solution is to insert a resistive core in the cable - this allows to control interstrand resistance, breaking the loops. Little experience has been acquired on winding cored cables, even though the few results are encouraging [22]. Cored cables have shown to be effective also for avoiding a degradation of performance with high ramp rates.

VII. Towards 20 T

The above considerations suggest that to move towards a 20 T operational field one needs an HTS superconductor:

- Able of carrying 400 A/mm^2 overall current density in operational conditions above 20 T;
- Without significant stress degradation up to 200 MPa (or larger …);
- With a filament size of the order of 10 μm;
- Available in Rutherford cable; this last requirement is controversial since one could explore other possibilities (for instance, Roebel cable).

Today Bi-2122, which is below of at least a factor two for current density, is available in Rutherford cables but has a large degradation with strain (see Fig. 14). The alternative YBCCO has a much larger current density and a good resistance to stress but it is not available in cables. In both cases the price is also a major issue. Having long cable lengths is also an important manufacturing issue.

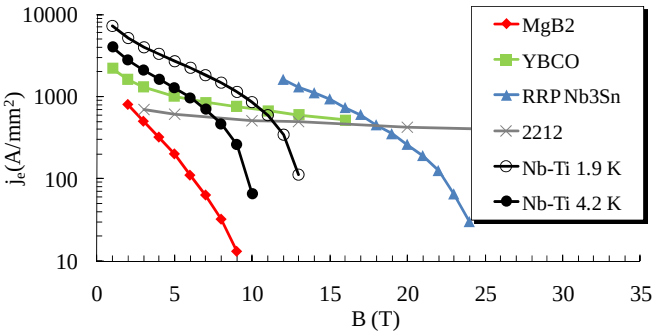

Fig. 13: Critical current in the superconductor [23].

VIII. Performance

In Fig. 14 we summarize the performance of the Nb-Ti and Nb_3Sn dipoles, plus the Nb_3Sn quadrupoles made for the LARP. We plot the maximum achieved peak field in the coil after training, allowing a direct comparison between dipoles and quadrupoles, and a guess percentage of short sample reached. Remember that this field is not usable, since it is in the coil. The comparison is not totally fair since some magnets have been tested at 1.9 K, and others only around 4 K. Anyway, Nb_3Sn clearly proves its potential to overcome the 10 T barriers and to reach 15 T in the coil.

The criteria to judge the performance of a magnet are always widely debated. We report the opinion of a recent discussion triggered by the LHC upgrade [24], stating that a good performance is given by three factors:

- Rapidly reaching nominal current (without or with one quench);
- Showing the ability to reach maximum performance, (90% of short sample with "a few" quenches);
- Showing the ability of keeping the training (no quenches after a thermal cycle to reach nominal).

These are criteria for magnets which are present in the accelerator in several tens of units: the criteria can be relaxed if one has only a few units in the machine, i.e. one can withstand some training after installation.

Nb_3Sn made impressive progress in the past years but there are still some issues, namely

- In general, a longer training w.r.t. Nb-Ti in the range 80-90% of short sample;
- In many cases the additional 10% provided by 1.9 K w.r.t. 4.2 K is not reached, or it is only partially reached. Instabilities are considered as the main source, and smaller filament size and high residual resistivity ratio should help in reducing them.
- The scaling in length from 1 m to 3.4 m has been proven on one magnet [25], but more statistics and experience should be gathered. Longer lengths make some aspects of coil manufacturing much more critical – in particular all issues related to thermal contraction and different mechanical properties of the different materials. Finally, another factor three is needed to go from 3.4 to 10 m.

Exciting research programs with ambitious goals are set in in the US, Europe and Japan for this decade, the LHC luminosity upgrade [26] being the major test bench for the application of these technologies. In a few years the community will be able to establish if magnets in the range of 10-15 T can operate in an accelerator, and if there is hope to approach the 20 T.

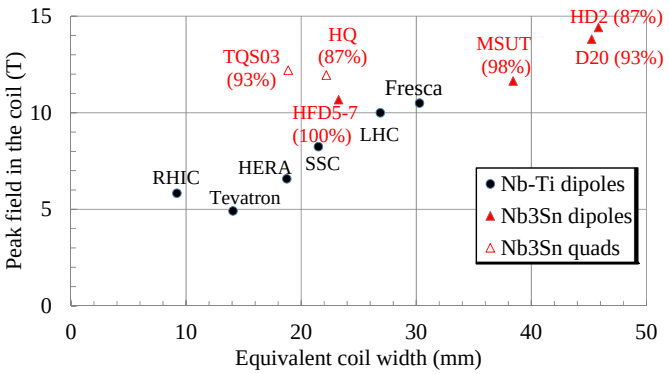

Fig. 14: Peak field in the coil reached after training versus equivalent coil width. Estimate of the percentage of short sample between brackets for Nb_3Sn magnets.

Acknowledgements

We wish to thank B. Bordini and P. P. Granieri for estimates of the energy margin, and we acknowledge L. Bottura, P. Fessia, A. Milanese, G. de Rijk and L. Rossi for reading the manuscript and useful comments.

REFERENCES

[1] P. Ferracin, et al., "Recent test results of the high field Nb_3Sn dipoles magnet HD2", *IEEE Trans. Appl. Supercond*.,Vol. 20, pp. 292-5, (2010).

[2] J. Billan, et al., "Construction of a prototype superconducting quadrupole magnet for a high-luminosity insertion at the CERN Intersecting Storage Ring", *CERN Yellow Report* 1976-016, (1976).

[3] W. E. Cooper, et al., *Fermilab Report* TM-1183 (1983).

[4] J. Schwartz, "Status of high temperature superconductor based magnets and the conductors they depend on", CERN Yellow Report 2011-3 (2011) 59-69.

[5] L. Bottura, "A practical fit for the critical surface of Nb-Ti", *IEEE Trans. Appl. Supercond*.,Vol. 10, pp. 1054-7, (2000).

[6] L. T. Summers, et al., "A model for the prediction of Nb3Sn critical current as a function of field, temperature, strain and radiation damage", *IEEE Trans. Magnetics*,Vol. 27, pp. 2041-4, (1991).

[7] A. Devred, "Practical low-temperature superconductors for electromagnets", *CERN Yellow Report* 2004-006, (2004).

[8] B. Bordini, P. Granieri and P. Ferracin, private communication.

[9] S. Caspi, et al., "Test results of 15 T Nb_3Sn quadrupole magnet HQ01 with a 120 mm bore for the LHC luminosity upgrade", *IEEE Trans. Appl. Supercond*.,Vol. 21, pp. 1854-7, (2011).

[10] L. Rossi, E. Todesco, "Electromagnetic design of superconducting dipoles based on sector coils", *Phys. Rev. STAB* **10** 112401 (2007).

[11] L. Rossi, E. Todesco, "Electromagnetic design of superconducting quadrupoles", *Phys. Rev. STAB* **9** 102401 (2006).

[12] D. Dietderich, et al., "Critical current of superconducting Rutherford cable in high magnetic field with transverse pressure", *IEEE Trans. Appl. Supercond.*, Vol. 9, pp. 122-5, (1999).

[13] G. De Rijk, these proceedings

[14] D. Dietderich, et al., "Cable R&D for the LHC accelerator research program", *IEEE Trans. Appl. Supercond.*, Vol. 17, pp. 1481-4, (2007).

[15] E. Barzi, "Effect of transverse pressure on brittle superconductors", *IEEE Trans. Appl. Supercond.*, Vol. 18, pp. 980-3, (2008).

[16] H. Felice, et al., "Test results of TQS03: a LARP shell-based Nb_3Sn quadrupole using 108/127 conductor", *J. Phys. Conf. Series*, Vol. 234, 032010, (2010).

[17] P. Fessia, et al., "Parametric analysis of forces and stresses in superconducting dipoles", *IEEE Trans. Appl. Supercond.*, Vol. 19, pp. 1203-7, (2009).

[18] P. Fessia, et al., "Parametric analysis of forces and stresses in superconducting quadrupole sector windings", *IEEE Trans. Appl. Supercond.*, Vol. 17, pp. 1269-72, (2007).

[19] A. F. Lietzke, et al., "Test results for a Nb3Sn dipole magnet", *IEEE Trans. Appl. Supercond.*, Vol. 7, pp. 739-42, (1997).

[20] B. Bordini. L. Rossi, "Self-field instability in high-jc Nb_3Sn strands with high copper residual resistivity ratio", *IEEE Trans. Appl. Supercond.*, Vol. 19, pp. 2470-6, (2009).

[21] A. Zlobin, et al., "Effect of flux jumps in superconducting accelerator magnet performance", *IEEE Trans. Appl. Supercond*.,Vol. 16, pp. 1308-11, (2006).

[22] G. Chlachidze, et al., "The study of single Nb_3Sn quadrupole coils using a magnetic mirror", *IEEE Trans. Appl. Supercond*.,Vol. 21, pp. 1692-5, (2011).

[23] P. Lee, private communication.

[24] G. De Rijk, private communication.

[25] G. Ambrosio, et al., "Test results of the first 3.7 m long Nb3Sn quadrupole by LARP and future plans", *IEEE Trans. Appl. Supercond.*, Vol. 21, 1858-62 (2011).

[26] L. Rossi, these proceedings.

[27] L. Rossi, E. Todesco, "Conceptual design of 20 T dipoles for High-Energy LHC", CERN Yellow Report 2011-3 (2011) 13-19.